1774–1788 *Nucleic Acids Research, 2011, Vol. 39, No. 5* *Published online 3 November 2010*
doi:10.1093/nar/gkq1083

Direct involvement of the TEN domain at the active site of human telomerase

Julie Jurczyluk[1,2], Amanda S. Nouwens[1,2], Jessica K. Holien[3], Timothy E. Adams[4], George O. Lovrecz[4], Michael W. Parker[3], Scott B. Cohen[1,2] and Tracy M. Bryan[1,2,*]

[1]Children's Medical Research Institute, Westmead, NSW 2145, [2]Faculty of Medicine, University of Sydney, NSW 2006, [3]Biota Structural Biology Laboratory, St Vincent's Institute of Medical Research, Fitzroy, VIC 3065 and [4]Commonwealth Scientific and Industrial Research Organisation Molecular and Health Technologies, Parkville, VIC 3052, Australia

Received June 24, 2010; Revised October 14, 2010; Accepted October 18, 2010

ABSTRACT

Telomerase is a ribonucleoprotein that adds DNA to the ends of chromosomes. The catalytic protein subunit of telomerase (TERT) contains an N-terminal domain (TEN) that is important for activity and processivity. Here we describe a mutation in the TEN domain of human TERT that results in a greatly increased primer K_d, supporting a role for the TEN domain in DNA affinity. Measurement of enzyme kinetic parameters has revealed that this mutant enzyme is also defective in dNTP polymerization, particularly while copying position 51 of the RNA template. The catalytic defect is independent of the presence of binding interactions at the 5′-region of the DNA primer, and is not a defect in translocation rate. These data suggest that the TEN domain is involved in conformational changes required to position the 3′-end of the primer in the active site during nucleotide addition, a function which is distinct from the role of the TEN domain in providing DNA binding affinity.

INTRODUCTION

Telomeres, the protective cap on the end of linear eukaryotic chromosomes, are composed of short G-rich DNA repeats bound by sequence-specific proteins (1). The telomeres of unicellular eukaryotes and of the germ cells of multicellular organisms are maintained by the ribonucleoprotein enzyme telomerase, which was first identified in the ciliated protozoan *Tetrahymena thermophila* (2). Telomerase activity has been detected in ~90% of human cancers, providing a telomere maintenance mechanism that is necessary for their unlimited growth (3–5).

The catalytic protein subunit of telomerase, telomerase reverse transcriptase [TERT (6)], contains protein motifs that are conserved with other reverse transcriptases ('RT motifs') and motifs in its amino terminal region that are conserved among TERTs from different species. A defined region of the telomerase RNA subunit is used as the template for addition of DNA repeats onto telomeres (7). A complex consisting of TERT and telomerase RNA is sufficient to reconstitute *in vitro* telomerase activity from *Tetrahymena* and human enzymes, measured by processive extension of a DNA oligonucleotide with telomeric DNA repeats (8,9). The repeated cycling of reverse transcription from a short segment of RNA, followed by translocation to the beginning of this sequence, leads to the unique property of telomerase known as 'repeat addition processivity'.

There is evidence for telomerase from several species that there are multiple sites of interaction with different regions of the DNA primer. For example, the affinity of *Tetrahymena* telomerase for DNA decreased in a stepwise manner as the primer was reduced in length from 18 to 12 nt then 6 nt (10,11), and two 5′-regions of a 24 nt primer influenced yeast telomerase activity (12). Sequences at the 5′-end of the primer also affected the processivity of endogenous human and *Tetrahymena* telomerase (13,14). These observations led to the proposal that telomerase contains a DNA-binding site outside the template region, called the 'anchor site' (13–15). It was proposed that the anchor site is necessary for repeat addition processivity, by allowing the enzyme to remain bound to the 5′-end of its DNA substrate during translocation. Thus, in order to fully understand the unique mechanism of telomerase, it is necessary to know more about the nature of the anchor site.

*To whom correspondence should be addressed. Tel: +61 2 8865 2909; Fax: +61 2 9687 2120; Email: tbryan@cmri.org.au
Present address:
Amanda S. Nouwens, School of Chemistry and Molecular Biosciences, University of Queensland, QLD 4072, Australia.

The N-terminal 200 amino acids of TERT [known as region I (16) or the GQ (17), RID1 (18) or TEN (19) domain] have been proposed as a key contributor to the telomerase anchor site. This region of TERT has the ability to form a soluble, protease-resistant, independently-folded structure (17,19–21). Complementation studies with fragments of human TERT indicate that this region (together with an adjacent linker domain) can interact *in trans* with the rest of the TERT protein (18,22–24). Activity-based assays have provided support for anchor site functions (25–27). Direct evidence for the involvement of this region in DNA binding was provided by the demonstration that mutations in *Tetrahymena* TEN led to decreased crosslinking to a primer containing 5-iodo-deoxyuridine (5-iodo-dU) substitutions at its 5′-end (19), and the site of crosslinking to a short primer was mapped to a particular amino acid within TEN (W187) (28). Direct binding assays (using capture with a biotinylated primer or gel shift analysis) have demonstrated that a fragment of human TERT encompassing TEN can bind telomeric DNA primers (24,29,30).

The exact role of the TEN domain in DNA binding, however, remains uncertain. Its affinity for DNA appears to be relatively low compared to other regions of TERT (11); a recent study using a bacterially-expressed TEN fragment of hTERT in gel shift analyses was unable to produce enough protein to quantitatively measure DNA affinity (24), implying a low-affinity interaction. Also, amino acids in TEN critical for repeat addition processivity or activity (L14 in *Tetrahymena* TERT and Q169 in hTERT, respectively) have been shown to not affect affinity with DNA of the same length as used in the activity assays (24,31). However, the amino acid corresponding to Q169 in *Tetrahymena* TERT (Q168) is involved in crosslinking to DNA (19); it is not clear if this discrepancy is due to a species difference or a difference in assays used to measure binding.

Given this uncertainty, we set out to quantitatively examine the effect on DNA binding of mutations in the hTERT TEN domain. We also examined the same mutations using activity assays, carrying out a detailed analysis of telomerase kinetic parameters in order to define the reason for reduced activity. Our data suggest that amino acids within the TEN domain are involved in positioning the 3′-end of the primer in the active site during nucleotide addition, a function which is distinct from the role of the TEN domain in providing DNA binding affinity.

MATERIALS AND METHODS

Plasmids and oligonucleotides

A panel of hTERT mutants with substitutions of the sequence NAAIRS and an N-terminal FLAG tag in the retroviral vector pBabehygro was kindly provided by Dr Christopher Counter, Duke University Medical Centre, Durham, NC (32). To create plasmids for *in vitro* expression, selected mutants were digested with EcoRI/SalI and the FLAG-hTERT fragment was sub-cloned into EcoRI/SalI sites of the pET-28 plasmid (Invitrogen). After carrying out many of the experiments in this study, we discovered two variations in the hTERT sequence in the NAAIRS panel compared to the hTERT sequence in Genbank entry AF015950 (33–35). These hTERT sequence changes (S229T and D516G) were corrected in the wild-type (wt) and mutant +170 expression constructs using the QuikChange II XL site-directed mutagenesis kit (Stratagene). There was no significant difference between these sequence variants in any of the *in vitro* kinetic parameters measured in this study (Supplementary Table S1 and Figure S2).

To construct a plasmid for *in vitro* transcription of hTR, the hTR gene [nucleotides 1–592] was amplified by PCR (36) and inserted into the vector pGEM-T (Promega). The insert of this plasmid was reamplified using primers that covered the 451 nt of hTR and included a T7 promoter (5′-end, for transcription) and a FokI restriction sequence (3′-end, for plasmid linearization) and inserted into the EcoRI/BamHI sites of plasmid pUC19. Linearization of the plasmid with FokI results in a transcription product terminating at the hTR 3′-end.

All oligonucleotides used for this study (listed in Table 1) were purchased from Sigma-Genosys in desalted lyophilized form and were gel purified on 20% acrylamide/8M urea gels before use. Purified oligonucleotides were resuspended in 10 mM Tris–Cl, pH 7.5.

In vitro translation and reconstitution of human telomerase

Human telomerase RNA was transcribed *in vitro* from the plasmid pUC-hTR as described earlier (37). The RNA was gel purified and quantitated by absorbance at 260 nm before use in *in vitro* translation reactions using the FLAG-hTERT-pET-28 plasmids described above. Translations were carried out using the TnT Quick for PCR rabbit reticulocyte lysate system (Promega). Recombinant enzyme reconstitution reactions (400 µl) contained 320 µl TnT Quick mastermix, 8 µg of plasmid encoding the protein, 32 µl of [^{35}S]methionine (Perkin-Elmer; 1175 Ci/mmol, 10 µCi/µl) and 150 nM telomerase RNA and were incubated at 30°C for 1 h. Reconstituted enzyme was immunopurified with anti-FLAG M2 affinity agarose beads (Sigma-Aldrich) in Protein LoBind tubes (Eppendorf). Beads (200 µl 1:1 slurry) were initially washed four times in 880 µl of Tris–IP buffer [10 mM Tris–Cl, pH 7.5, 100 mM KCl, 1 mM $MgCl_2$, 10% glycerol and 0.1 mM dithiothreitol (DTT)], centrifuging at 1000*g* for 2 min at 4°C between washes. The translation reaction was diluted 1:10 in Tris–IP buffer. The washed anti-FLAG beads were added and the sample rotated at 12 rpm at 4°C for 2 h. The beads were washed four times in 4 ml of hTel buffer (50 mM Tris–Cl, pH 8.0, 1 mM $MgCl_2$, 100 mM KCl, 5 mM DTT, 1 mM spermidine and 10% glycerol) before telomerase was eluted from the beads by competition with a 3× FLAG peptide (Sigma-Aldrich). The beads were resuspended in 120 µl of an elution mix (0.75 mg/ml FLAG peptide, 0.5 mg/ml BSA in hTel buffer) and rotated at 4°C for 1 h, centrifuged at 1000*g* for 2 min at 4°C and the eluate removed to a fresh LoBind tube.

Table 1. Oligonucleotides used in this study

Name	Sequence
18GGG	TTAGGGTTAGGGTTAGGG
18GGT	TAGGGTTAGGGTTAGGGT
18GTT	AGGGTTAGGGTTAGGGTT
18TTA	GGGTTAGGGTTAGGGTTA
18TAG	GGTTAGGGTTAGGGTTAG
18AGG	GTTAGGGTTAGGGTTAGG
18ACT	GGTTAGGGTTAACTTTAG
9GGG	GGGTTAGGG
5TTA	GGTTA
5GGT	AGGGT
Bio-18GGG	Biotin-CTAGACCTGTCATCATTAGGGTTAGGG TTAGGG
Bio-18TAG	Biotin-CTAGACCTGTCATCAGGTTAGGGTTAG GGTTAG
Bio-12GGG	Biotin-CTAGACCTGTCATCATTAGGGTTAGGG
Bio-PBR	Biotin-AGCCACTATCGACTACGCGATCAT
Telo4	CGGTGGAAGGCGGCAGGCCGAGGC

All sequences are listed 5′–3′.

The yield of active enzyme was determined by dot blotting using a probe against hTR. Aliquots of the immunopurified enzyme in formamide loading buffer (90% deionized formamide, 0.1% bromophenol blue, 0.1% xylene cyanol, in 1× TBE (89 mM Tris, 89 mM Boric acid, 2 mM EDTA)) were heated to 70°C for 10 min and chilled on ice for 2 min. The samples were dotted onto Hybond N+ membrane (GE Healthcare). The membrane was air dried for 1 h at RT, cross-linked with 254 nm UV light using the autocrosslink function of the Stratalinker cross-linker (Stratagene) and pre-hybridized in Church buffer [1% BSA (Fraction V grade, Roche), 1 mM EDTA, pH 7.5, 500 mM Na_2HPO_4, pH 7.2, 7% SDS] for 1 h at 55°C. The blot was hybridized in Church buffer overnight at 55°C with 1×10^7 cpm of ^{32}P end-labelled Telo4 probe directed against hTR (Table 1). The membrane was washed three times for 10 min in wash buffer (15 mM NaCl, 1.5 mM Tri-sodium citrate, 0.1% SDS) at RT, sealed in a plastic bag, exposed to a phosphorimager screen overnight, scanned with a Typhoon 9410 Workstation (GE Healthcare) and quantitated with ImageQuant software (Molecular Dynamics). Aliquots of purified recombinant enzyme were added to an equal volume of 5× Laemmli's sample buffer (250 mM Tris–Cl, pH 6.8, 10% SDS, 0.01% bromophenol blue, 50% glycerol, 1.8 M β-mercaptoethanol) and were also subjected to SDS–PAGE analysis in order to normalize yield of RNA to yield of hTERT. Samples were heated to 100°C for 3 min and electrophoresed on an 8% polyacrylamide/SDS gel. The gel was fixed in 25% isopropyl alcohol, 10% acetic acid, 20% glycerol for 30 min, dried at 80°C for 1 h and exposed to a phosphorimager screen overnight.

Cell culture and plasmid transfection

WI-38 VA13/2RA human foetal fibroblasts (ATCC) and human embryonic kidney (HEK) cell line 293T were cultured in Dulbeco's Modified Eagles Medium (Invitrogen) supplemented with 10% foetal calf serum (Sigma) and grown in a 37°C humidified incubator containing 5% CO_2.

WI-38 VA13/2RA and 293T cells were co-transfected with plasmids encoding hTERT under a CMV promoter (38) and hTR under a U3 promoter (39) using Fugene-6 transfection reagent (Roche) and incubated at 37°C for 6 h. After 72 h at 32°C the cells were harvested and lysed in 1 ml of buffer A per 10^7 cells (20 mM HEPES–KOH, pH 7.9, 300 mM KCl, 2 mM $MgCl_2$, 10% glycerol, 1 mM EDTA, 0.1% Triton X-100, 1 mM DTT and 1 mM PMSF). The cell suspensions were rotated at 4°C for 1 h and centrifuged at 18 000*g* at 4°C for 20 min to clarify the lysate. The supernatant was transferred to a Protein LoBind microfuge tube (Eppendorf), snap frozen in liquid nitrogen and stored at −80°C.

Immunopurification of overexpressed or endogenous telomerase

Lysates of telomerase-transfected WI-38 VA13/2RA or 293T cells (10^7 cells in 1 ml; described above) or untransfected 293 cells (5×10^7 cells in 1 ml) were incubated with 20 μg sheep polyclonal anti-hTERT antibody (40) for 1 h at 4°C. Protein G agarose beads (50 μl) were pre-blocked in buffer A + BSA (0.5 mg/ml) for 30 min at RT, added to the sample and rotated for 1 h at 4°C. The remaining steps of the protocol were conducted in a 4°C coldroom with ice-cold buffers. Samples were transferred into Illustra Micropsin columns (GE Healthcare) attached to a vacuum manifold and were washed with 10 ml of buffer A followed by 5 ml of hTel buffer (50 mM Tris–Cl, pH 8.0, 1 mM $MgCl_2$, 100 mM KCl, 5 mM DTT, 1 mM spermidine, 10% glycerol). To elute the purified protein, 300 μl of hTel buffer containing 50 μM peptide antigen (40) was added to the plugged column and rotated at RT for 1 h. The microspin column was unplugged and centrifuged at 1000*g* for 1 min at RT to collect the enzyme into a Protein LoBind tube (Eppendorf). Purified enzyme was snap frozen in liquid nitrogen and stored at −80°C. The yield of active enzyme was determined by dot blotting using a probe against hTR, as described above.

Telomerase activity assays

Telomerase activity was measured by incubating 10 μl of immunopurified telomerase (recombinant, endogenous or overexpressed) in a 20 μl reaction including 50 mM Tris–Cl, pH 8.0, 1 mM $MgCl_2$, 50 mM KCl, 5 mM DTT, 1 mM spermidine, 10% glycerol, 0.5 mM dTTP, 0.5 mM dATP, 4.6 μM nonradioactive dGTP and 0.33 μM [α-^{32}P]dGTP at 20 mCi/ml, 6000 Ci/mmol (PerkinElmer Life Sciences). The indicated DNA primers were added to the reactions at concentrations of 10 nM to 5 μM. Standard primer concentrations were 1–2 μM for 18-nt primers, 5 μM for 9-nt primers and 50 μM for 5 nt primers. The reactions were incubated at 30°C for 1–6 h; the linear phase of enzyme activity extends for ∼10 h (data not shown). Reactions were terminated by addition of 100 μl of TES buffer (50 mM Tris–Cl, pH 8.3, 20 mM EDTA, 0.2% SDS); 1000 cpm of a ^{32}P end-labelled 100-nt oligonucleotide

was added as a recovery and loading control. The reaction products were phenol/chloroform extracted and ethanol precipitated. The pellet was resuspended in 5 µl of TE buffer and 5 µl of formamide loading buffer (90% deionised formamide, 0.1% bromophenol blue, 0.1% xylene cyanol in 1× TBE). Immediately prior to gel loading, samples were heated to 70°C for 5 min and chilled on ice for 2 min before centrifuging at 16 000*g* at 4°C for 2 min. Half the reaction was electrophoresed on a denaturing 10% polyacrylamide/8 M urea sequencing gel for 2 h at 80 W. The gel was dried at 80°C for 30 min, exposed to a phosphorimager screen, scanned with a Typhoon 9410 Workstation and quantitated with ImageQuant software.

For experiments using a single nucleotide, the concentrations of nucleotide were 47.5 µM non-radioactive dTTP and 2.5µM [α-^{32}P] dTTP at 10 mCi/ml, 800 Ci/mmol (for 'T-only' assays), 47.5 µM non-radioactive dATP and 2.5µM [α-^{32}P] dATP at 10 mCi/ml, 800 Ci/mmol (for 'A-only' assays) and 10 µM non-radioactive dGTP and 0.66 µM [α-^{32}P] dGTP at 20 mCi/ml, 6000 Ci/mmol (for 'G-only' reactions). These concentrations are above the approximate K_m of wt recombinant telomerase for each nucleotide [8 µM for dTTP, 1 µM for dATP (data not shown) and 1.3 µM for dGTP]. Experiments measuring the affinity of dGTP included 0.5 mM dTTP, 0.5 mM dATP and the indicated concentration of dGTP at a constant specific activity of 200 Ci/mmol.

The intensity of extension products at each substrate concentration was summed and normalized against the intensity of the ^{32}P-labelled 100-nt oligonucleotide loading control to give relative activities; those in Figure 1c were carried out at 1 µM substrate. These data were then expressed as a percentage of the reaction with maximal activity and plotted against oligonucleotide (substrate) concentration [*S*]. The curve was fitted to the equation $y = (V_{max} \times [S])/(K_m + [S])$, to yield the Michealis–Menton affinity constant K_m. To calculate relative processivity, the intensity of the first 3–5 repeats was adjusted for specific activity (i.e. number of incorporated radiolabelled nucleotides per repeat) and plotted versus repeat number on a log-linear graph. Processivity was defined as $-0.693/s$, where s is the slope of the resulting straight line.

For calculating k_{obs}, gels such as that in Figure 6b included a standard curve of known amounts (cpm) of a ^{32}P-labelled 100-nt oligonucleotide. The cpm of each telomerase product band were converted to Ci (since 1 cpm = 2.2×10^{-12} Ci for ^{32}P), then to fmol based on the specific activity of the radiolabelled nucleotides, and normalized to the fmol of enzyme used in the assay to give k_{obs}.

DNA binding assay to measure primer binding to hTERT

Ultralink Immobilized NeutrAvidin Protein Plus beads (Thermo Scientific) (700 µl) were washed four times in 1 ml wash buffer 75 (50 mM Tris–Cl, pH 8.0, 1 mM $MgCl_2$, 10% glycerol, 75 mM KCl, 5 mM DTT, 1 mM spermidine), centrifuging at 1000*g* for 1 min at 4°C between washes. The beads were incubated twice with 1 ml of blocking buffer (50 mM Tris–Cl, pH 8.0, 1 mM $MgCl_2$, 10% glycerol, 75 mM KCl, 5 mM DTT, 1 mM spermidine, 0.75 mg/ml BSA, 0.15 mg/ml glycogen) for 30 min at RT with agitation and resuspended in 350 µl blocking buffer (for 293T telomerase) or hTel buffer (for recombinant telomerase). Immunopurified overexpressed telomerase from 293T cells (50 µl) or immunopurified recombinant telomerase (10 µl) was added to a 100 µl reaction including hTel buffer (50 mM Tris–Cl, pH 8.0, 1 mM $MgCl_2$, 50 mM KCl, 5 mM DTT, 1 mM spermidine, 10% glycerol) and oligonucleotide at concentrations ranging from 0 to 10 µM. Similar results were obtained with telomerase expressed in 293T cells or WI-38 VA13/2RA cells (data not shown). The reactions were incubated at 30°C for 30 min (293T telomerase) or 60 min (recombinant telomerase) followed by the addition of 50 µl of blocked NeutrAvidin beads and agitation at 4°C for 2 h. The samples were washed three times in 300 µl of wash buffer 50 (50mM Tris–Cl, pH 8.0, 1 mM $MgCl_2$, 10% glycerol, 50 mM KCl, 5 mM DTT, 1 mM spermidine) with centrifugation at 1000*g* for 2 min at 4°C between washes, before the bead pellets were resuspended in 100 µl of formamide loading buffer (see above) containing 0.5 mM biotin. Immediately prior to dot blotting, the samples were heated to 70°C for 10 min, chilled on ice for 2 min and centrifuged at 14 000*g* for 1 min at 4°C. Half of the reaction was dotted onto Hybond N+ membrane alongside *in vitro* transcribed hTR standards loaded in an equal volume of formamide loading buffer. The membrane was probed with ^{32}P end-labelled Telo4 probe against hTR, as described above. The blot was exposed to a phosphorimager screen for 72 h and analysed using ImageQuant TL software. The signal from the sample blank (containing no oligonucleotide) representing background binding to the beads was substracted from all others. The resulting value was expressed as a percentage of the maximal intensity at the highest primer concentration and plotted against oligonucleotide (substrate) concentration [*S*]. The curve was fitted to the following equation: $y = (B_{max} \times [S])(K_d + [S])$, where B_{max} is the maximal level of binding, to yield the dissociation constant K_d.

Glycerol density gradient centrifugation and fractionation

Glycerol gradient stock solutions containing either 10 or 40% glycerol in 300 mM KCl, 2 mM $MgCl_2$, 0.1% Triton X-100, 1 mM DTT and 20 mM HEPES–KOH pH 7.9 were combined using a two-chamber gradient mixer to pour 11 ml of 10–40% linear glycerol density gradients in Ultra-Clear 13.2 ml centrifuge tubes (14 × 89 mm; Beckman Coulter). Recombinant wild type or +170 mutant telomerase (500 µl), synthesized in rabbit reticulocyte lysate as described above, was applied to the top of the gradient. Centrifugation was performed with a SW-41 Ti swinging-bucket rotor (Beckmann Coulter) at 230 000*g* at 4°C for 24 h. Following centrifugation, glycerol gradients were collected by puncturing the base of each tube with a 30-gauge needle; 23 0.5 ml fractions were collected by gravity elution and stored at −80°C. Telomerase activity was measured using 27 µl of each glycerol

gradient fraction in a 40 µl reaction using 1 µM of primer Bio-18GGG, as described above.

Northern blotting

Purified telomerase (from 5×10^6 telomerase-transfected WI-38 VA13/2RA cells) in 300 µl buffer A was digested with 33 µl Proteinase K buffer (100 mM Tris–Cl, pH 7.5, 75 mM EDTA, 6% SDS) and 2 µl proteinase K (40 µg) for 2 h at 45°C. The samples were spiked with 5000 cpm of a ^{32}P-labelled 100-nt oligonucleotide as a recovery and loading control, phenol/chloroform extracted and ethanol precipitated. The pellet was resuspended in 10 µl of MilliQ water and 10 µl formamide loading buffer (90% deionized formamide, 0.1% bromophenol blue, 0.1% xylene cyanol in 1× TBE). Samples were heated at 70°C for 5 min, cooled on ice for 2 min and electrophoresed on a 1.5-mm-thick 4% polyacrylamide, 8 M urea, 1× TBE gel for 1 h at 25 W in 1× TBE buffer. The gel was transferred onto Hybond XL membrane (GE Healthcare) by electroblotting for 2 h at 1.5 A in 0.5× TBE buffer cooled to 4°C with a recirculating water bath. The membrane was probed with ^{32}P end-labelled Telo4 probe directed against hTR, as described above.

Western blotting

Purified telomerase (from 5×10^6 telomerase-transfected WI-38 VA13/2RA or 293T cells) was added to an equal volume of 5× Laemmli's sample buffer (250 mM Tris–Cl, pH 6.8, 10% SDS, 0.01% bromophenol blue, 50% glycerol and 1.8 M β-mercaptoethanol) and heated to 95°C for 5 min. The samples were electrophoresed on an 8% polyacrylamide/SDS-PAGE gel in Laemmli's running buffer (25 mM Tris, 0.1% SDS, 192 mM glycine) for 2 h at 100 V and transferred to Hybond enhanced chemiluminescent (ECL) nitrocellulose (GE healthcare) by electroblotting in Transfer buffer (25 mM Tris, 0.01% SDS, 192 mM glycine) at 0.5 A for 1 h. The membrane was blocked for 1 h at RT in phosphate buffered saline (PBS) containing 2% skim milk and 0.05% Tween-20. The membrane was then incubated with primary antibody [goat polyclonal anti-hTERT (sc7215); Santa Cruz Biotechnology] diluted 1:1000 in PBS containing 1% skim milk and 0.05% Tween-20 overnight at 4°C. The membrane was washed for 1 h in several changes of PBS/0.05% Tween-20 at RT followed by incubation for 1 h at RT with the secondary antibody (rabbit anti-goat immunoglobulin horseradish peroxidase; DAKO) diluted 1:10 000 in 1× PBS containing 1% skim milk and 0.05% Tween-20. The membrane was rinsed with PBS before incubation with Amersham ECL plus Western blotting detection reagent (GE Healthcare) for 5 min at RT. The blot was exposed to a LASS-4000 Luminescent Image Analyser (FujiFilm) and quantitated using Multigauge software.

Protein homology modelling and nucleic acid docking

An homology model of the human hTERT TEN domain was determined by threading the TEN domain sequence of hTERT onto chain A of the *Tetrahymena* TEN domain crystal structure [PDB id:2B2A (19)] using the Bioinformatics Online Toolkit (http://toolkit.tuebingen.mpg.de). A 3D homology model was then constructed with MODELLER (http://www.salilab.org/modeller) and the top-ranked model minimized using the Tripos force field until a gradient consensus was reached (21 003 iterations, energy = −615.496 kcals/mol) followed by minimization using the Kollman-all atom force field, with the addition of AMBER charges until a gradient consensus was reached (16 957 iterations, energy = −2648.889 kcal/mol). The stereochemical quality of the model was checked with PROCHECK V3.5, with 96.9% of residues in an acceptable region of a Ramachandran plot and all other stereochemical statistics deemed reasonable (41).

The DNA primer 5′-TTA-3′ was constructed in Sybyl-X-1.1 using the Biopolymer module (http://www.tripos.com). The DNA single strand was docked into the TEN domain model using the HEX program [(42) and http://www.csd.abdn.ac.uk/hex/]. A shape and electrostatics correlation was used in the 3D Fastlite mode with a grid dimension of 0.75 Å, receptor and ligand range 180°, twist range 360°, distance range 40 Å and a scan step of 0.75. Two thousand solutions were requested in the initial dock with 20 clusters of solutions found after post-minimization. The complementary RNA base pairs (5′-UAA-3′) were added to the lowest energy dock and visually analyzed.

RESULTS

A mutant of the hTERT TEN domain with reduced activity and processivity, and dramatically increased primer K_m

To quantitate the contribution of human TEN to telomerase activity and DNA affinity, we performed *in vitro* assays with a panel of hTERT mutants with six amino acid substitutions of the sequence NAAIRS (32,43). This substitution is predicted to have minimal effect on protein structure (44). Telomerase was reconstituted in rabbit reticulocyte lysates (RRL) using hTERT substituted with NAAIRS at one of fifteen positions throughout the protein (Figure 1a), and activity measured with a direct (i.e. non-PCR) assay using oligonucleotide 18GGG [(TTAGGG)$_3$] as a substrate (Figure 1b; see Table 1 for oligonucleotide sequences). Relative activity levels were quantitated based on total product intensity, and repeat addition processivity (RAP) was determined from the rate of decrease of product intensity over the first three to five repeats (Figure 1c). As a first step towards examining DNA affinity, the K_m for primer 18GGG was measured by quantitating product intensity at different concentrations of this primer (Figure 1c).

Activity levels of most NAAIRS mutants reflected those measured using *in vivo* reconstituted telomerase (32,43). One exception is the mutation at amino acids 8–13 (hereafter called +8 in line with the previous nomenclature), which was substantially more active when reconstituted *in vitro* than *in vivo*. This may be explained by the observation that the extreme N-terminus of hTERT is involved in its nucleolar localization *in vivo* (45).

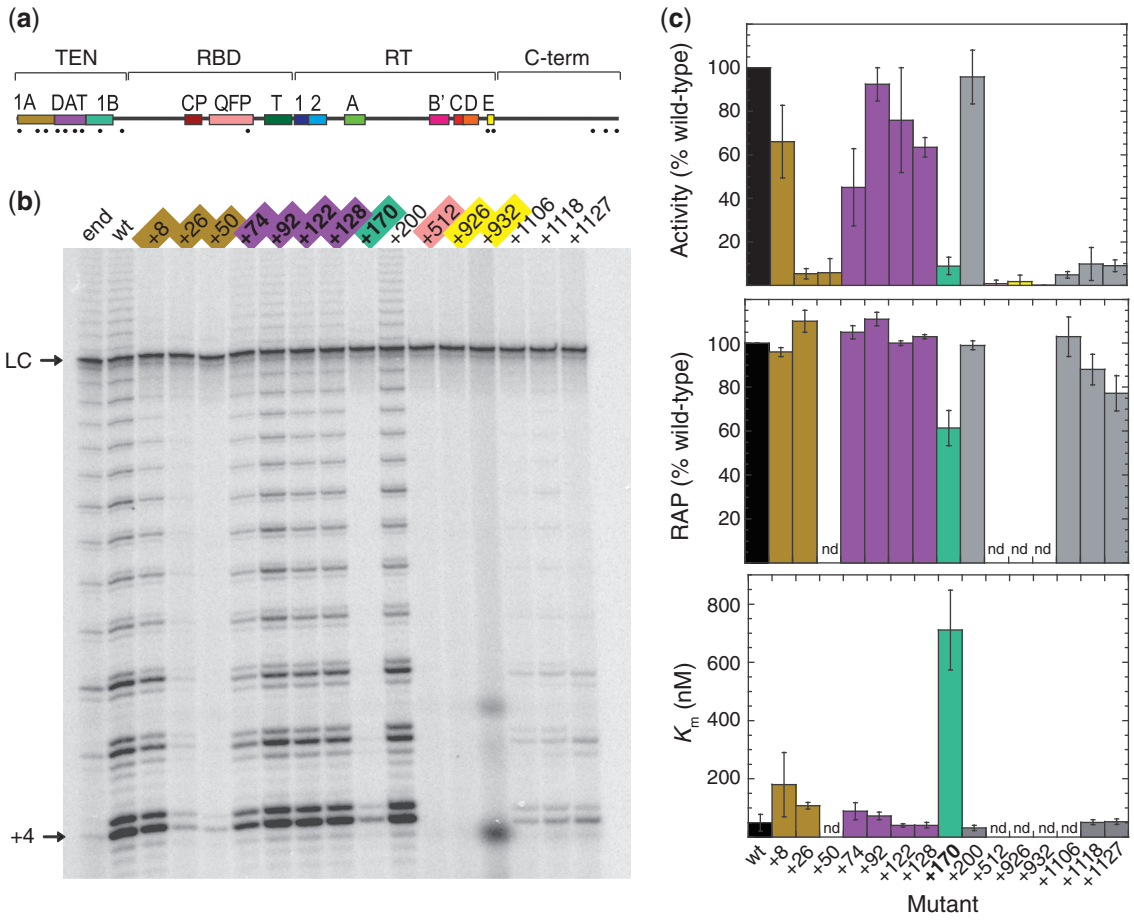

Figure 1. A mutant of the hTERT TEN domain with reduced activity and processivity, and dramatically increased primer K_m. (**a**) Schematic of the domain structure of hTERT, showing locations of the telomerase essential N-terminal domain (TEN), RNA binding domain (RBD), reverse transcriptase domain (RT) and C-terminal domain (C-term). Coloured boxes indicate conserved sequence motifs. Dots beneath the protein indicate locations of the fifteen NAAIRS substitutions examined in this study. (**b**) Direct telomerase activity assay of NAAIRS substituted telomerase reconstituted in rabbit reticulocyte lysates, and endogenous telomerase from 293 cells ('end'). LC: labelled 100 nt oligonucleotide as a recovery and loading control; +4: position of primer (18GGG) with the addition of 4 nt. (**c**) Quantitation of the relative activity, repeat addition processivity (RAP) and primer K_m (for 18GGG) of the panel of NAAIRS mutants. Values are the mean ± standard deviation of three independent experiments.

Table 2. K_m of various DNA primers with wt recombinant hTERT and mutant +170, and the fold difference between these numbers

Primer	Sequence	K_m (nM)			
		wt	+170	Fold difference	Endogenous wt
18GGG	$(TTAGGG)_3$	49 ± 29	710 ± 140	14	7.8 ± 0.3
18TTA	$(GGGTTA)_3$	65 ± 4	1530 ± 100	24	9.7 ± 5.6
9GGG	GGGTTAGGG	56 ± 16	300 ± 20	5	n.d.

The right column lists the K_m of some of the same primers for endogenous wt human telomerase. Results are the mean ± standard deviation of two to six experiments.
n.d., not determined.

A subregion of the TEN domain has been shown to be necessary for telomere extension *in vivo* but not telomerase activity, and has been called the dissociates activities of telomerase (DAT) domain (32). Mutations in the DAT domain (Figure 1, purple) had modest effects on activity and no reduction in RAP. Regions on either side of DAT (regions 1A and 1B) were much more important for activity. The 1B mutant (+170) had substantially reduced RAP, while the 1A mutants (+8, +26) had wt RAP. A mutation in the non-conserved linker region (+200) had no effect on activity or RAP, while the conserved motifs QFP and E [involved in RNA and DNA binding respectively (18,29)] were essential for activity. We confirmed that mutations in the hTERT C-terminus reduced both activity and RAP, as previously shown (43,46).

Analysis of the K_m for primer 18GGG gave unexpected results. Mutants +26, +74 and +92 showed very modest (~2-fold) increases in K_m, while the K_m of most other mutants did not differ from wt. The one exception was mutant +170 in region 1B, which had a dramatic (~14-fold) increase in K_m (Figure 1c, Table 2).

Primers with different permutations of the 3′-end have up to 100-fold differences in dissociation rate from endogenous human telomerase (47), accounting for the distinctive 6 nt pausing pattern of telomerase extension. Since the pausing pattern of recombinant human telomerase is

Table 3. K_d of various DNA primers with wt recombinant and overexpressed hTERT and mutant +170, and the fold difference between these numbers

Primer	K_d (nM)					
	Recombinant			Overexpressed in 293T		
	wt	+170	Fold difference	wt	+170	Fold difference
Bio-18GGG	164 ± 63	361 ± 142	2.2	0.5 ± 0.3	600 ± 70	1200
Bio-18TAG	n.d.	n.d.		0.9 ± 0.4	510 ± 90	567
Bio-12GGG	n.d.	n.d.		0.5 ± 0.1	1590 ± 770	3180

Results are the mean ± standard deviation of three to four experiments.
n.d., not determined.

very similar to that of endogenous telomerase purified from 293 cell extracts (Supplementary Figure S1), it is highly likely that recombinant telomerase shows the same pattern of dissociation at different template positions. We therefore also measured the K_m of the primer 18TTA [$(GGGTTA)_3$]; see Figure 6a for an illustration of the alignment of this primer with the RNA template relative to that of primer 18GGG. Mutant +170 showed an even greater increase in K_m with primer 18TTA (Table 2 and Supplementary Figure S1). For wt telomerase the K_m for primers 18GGG and 18TTA were not substantially different (Table 2); since these primers are predicted to have a ~100-fold difference in dissociation rate, this implies that K_m may not be a good reflection of primer affinity (K_d) for telomerase. This is also the case for endogenous human telomerase from 293 cells; the K_ms of 18GGG and 18TTA were lower for endogenous telomerase than recombinant, but were similar to each other (Table 2). We therefore embarked on an exploration of the kinetic parameters of mutant +170 telomerase in order to identify the defect(s) responsible for its dramatic K_m increase.

During the course of this study, we detected two additional amino acid mutations in the panel of NAAIRS mutants used (32) relative to a wt hTERT sequence in Genbank (33). We corrected these amino acids and confirmed that they have no effect on telomerase activity or on any of the kinetic parameters measured in this study (Supplementary Figure S2 and Table S1).

Mutant +170 has a defect in DNA binding affinity

Since the K_m for a primer-enzyme interaction (measured by activity) is not necessarily equal to the affinity constant (K_d) for the same interaction, we next measured primer affinity directly using a pulldown assay that we had developed for *Tetrahymena* telomerase (11). Biotinylated 18-nt telomeric primers were incubated with purified recombinant enzyme and recovered with Neutravidin beads, and the yield of telomerase measured by dot blot against hTR (Supplementary Figure S3). The K_d of primer binding to mutant +170 was only 2-fold greater than that of wt telomerase (Table 3), confirming that K_m is not a good measure of K_d for recombinant human telomerase.

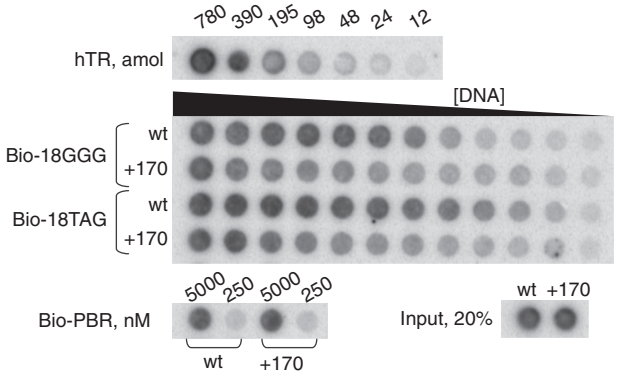

Figure 2. hTERT mutant +170 has a defect in DNA binding affinity. Biotinylated telomeric primers were incubated with wt or mutant telomerase reconstituted in 293T cells. The amount of telomerase recovered on NeutrAvidin beads was quantitated by dot blotting with a ^{32}P-labelled probe against hTR. The top row is a standard curve of *in vitro* transcribed hTR. The middle panel represents titrations of the indicated primers, at concentrations of 250, 50, 25, 5, 2.5, 1.25, 0.62, 0.31, 0.15 nM, 78, 39 and 0 pM (wt) or 5, 2.5, 1, 0.5, 0.25 μM, 50, 25, 5, 2.5, 1.25, 0.63 and 0 nM (+170). On the bottom left is binding of telomerase to a non-telomeric DNA control (Bio-PBR), and 20% of the input for each experiment is shown on the bottom right. Note that all panels are from the same exposure of a single dot blot, but are separated for ease of labelling.

Since endogenous human telomerase exhibits a lower K_m than recombinant enzyme (Table 2), we also measured direct primer binding affinities for endogenously-assembled human telomerase. We reconstituted wt and mutant +170 telomerase *in vivo* in 293T cells, purified it by immunopurification with an hTERT antibody (40) and employed the same direct primer binding assay. Under our transfection conditions in 293T cells, overexpressed telomerase activity exceeds the endogenous levels by ~200-fold, resulting in <1% contribution by the endogenous wt enzyme. To our surprise, the K_ds of primer binding of 18-nt primers to overexpressed cellular mutant +170 were 500–1200-fold greater than those of wt telomerase (Figure 2, Table 3). This indicates that recombinant human telomerase does not exactly recapitulate the DNA binding properties of the endogenously-assembled enzyme, and this discrepancy masks the dramatic defect in DNA binding affinity of mutant +170.

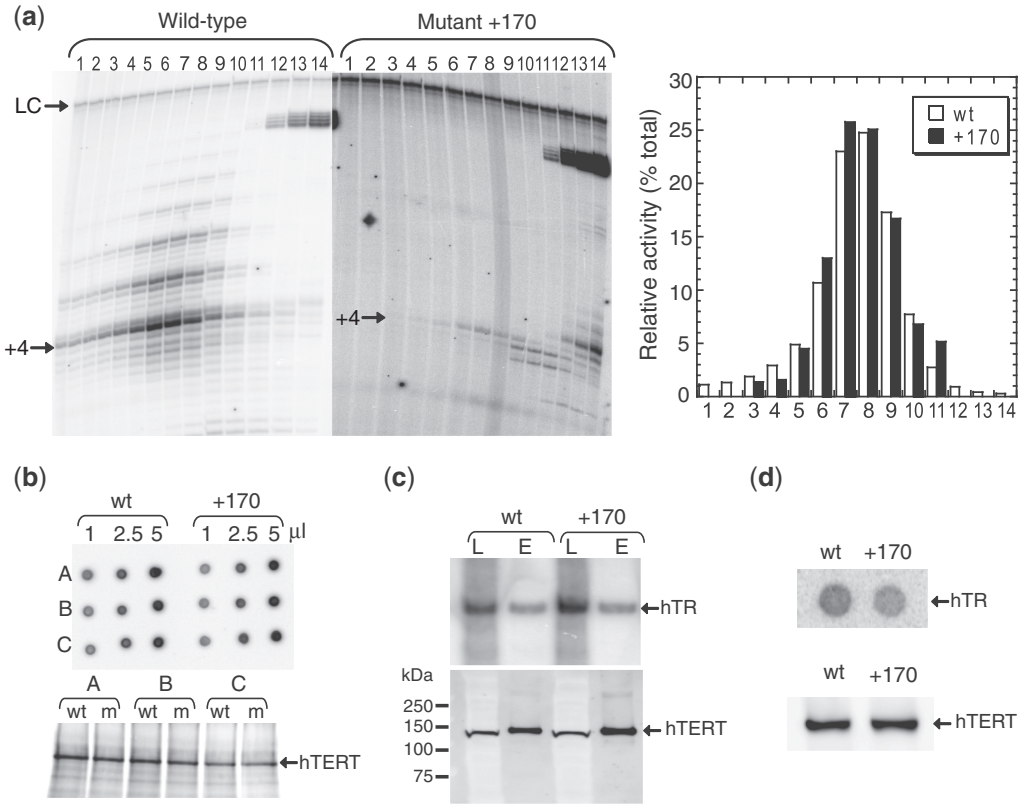

Figure 3. hTERT mutant +170 retains wt global structure. (**a**) wt and mutant telomerase reconstituted in rabbit reticulocyte lysates were fractionated over parallel 10–40% glycerol gradients, and the fractions subjected to a direct telomerase assay with primer 18GGG. The figure represents two different exposures of a single gel. LC: labelled 100 nt oligonucleotide as a recovery and loading control; +4: primer plus 4 nt. The relative activity in each fraction is plotted on the right. (**b**) Recombinant hTERT was immunoprecipitated with a FLAG tag antibody, and the recovery of hTR measured by dot blot with a probe against hTR (top panel). Triplicate experiments are shown (A–C). The bottom panel is an SDS–PAGE gel showing the yield of ^{35}S-labelled hTERT protein from each immunoprecipitate of wt or mutant +170 (m) telomerase. (**c**) WI38 VA13/2RA human fibroblasts were transfected with plasmids encoding hTR and wt or mutant hTERT. Telomerase was immunoprecipitated with an antibody against hTERT. Cell lysate (L) and purified enzyme (E) were electrophoresed on a northern blot for hTR (top panel) or a western blot for hTERT (bottom panel). (**d**) 293T human embryonic kidney cells were transfected with plasmids encoding hTR and wt or mutant hTERT. Telomerase was immunoprecipitated with an antibody against hTERT and detected on a dot blot for hTR (top panel) or a western blot for hTERT (bottom panel).

hTERT mutant +170 retains wt global structure

One potential explanation for the large effect of mutation +170 on K_m, K_d and processivity is an effect on enzyme structure. To rule this out, we fractioned wt and mutant +170 telomerase (reconstituted in RRL) over parallel glycerol gradients. The use of crude translation lysate resulted in products from contaminating polymerases and nucleases, some even more abundant than the extension products from mutant +170 (Figure 3a). Nonetheless, telomerase extension products from both enzymes were detected (Figure 3a, $n+4$ bands) and eluted with almost identical profiles (Figure 3a, right panel), indicating a similar overall composition and structure.

Another indicator of wt conformation is the ability to bind to hTR. This was measured by immunoprecipitation of *in vitro* translated hTERT with an antibody to an N-terminal tag, followed by dot blotting to quantitate yield of bound hTR (Figure 3b, top panel). When normalized to the yield of ^{35}S-labelled hTERT (Figure 3b, bottom panel), mutant +170 bound hTR at least as efficiently as wt hTERT (levels of 130 ± 10%). To measure the ability of mutant +170 hTERT to assemble with hTR within human cells, we also reconstituted wt and mutant telomerase in telomerase-negative WI38 VA13/2RA cells (which lack endogenous expression of hTERT and hTR). The amount of hTR that immunoprecipitated with mutant hTERT was equal to that with wt hTERT (Figure 3c; levels of 95 ± 19%), demonstrating that *in vivo* assembly of the telomerase complex was intact. Assembly of mutant +170 hTERT with hTR was slightly less efficient in 293T cells, at 63% of wt levels (Figure 3d).

Increased K_m of mutant +170 is not attributable to a defect in translocation rate or interaction with 5′-end of primer

It has been proposed that the effect of the TEN domain on RAP is due to a defect in the telomerase translocation step (31). It is difficult to directly measure translocation rate with a mutant that shows almost no detectable second repeat addition, so we instead examined the effect of mutant +170 on translocation indirectly. *In vitro* reconstituted telomerase was used to extend primer 18GGG in a reaction with ^{32}P-dTTP as the only nucleotide. This reaction results in the addition of two

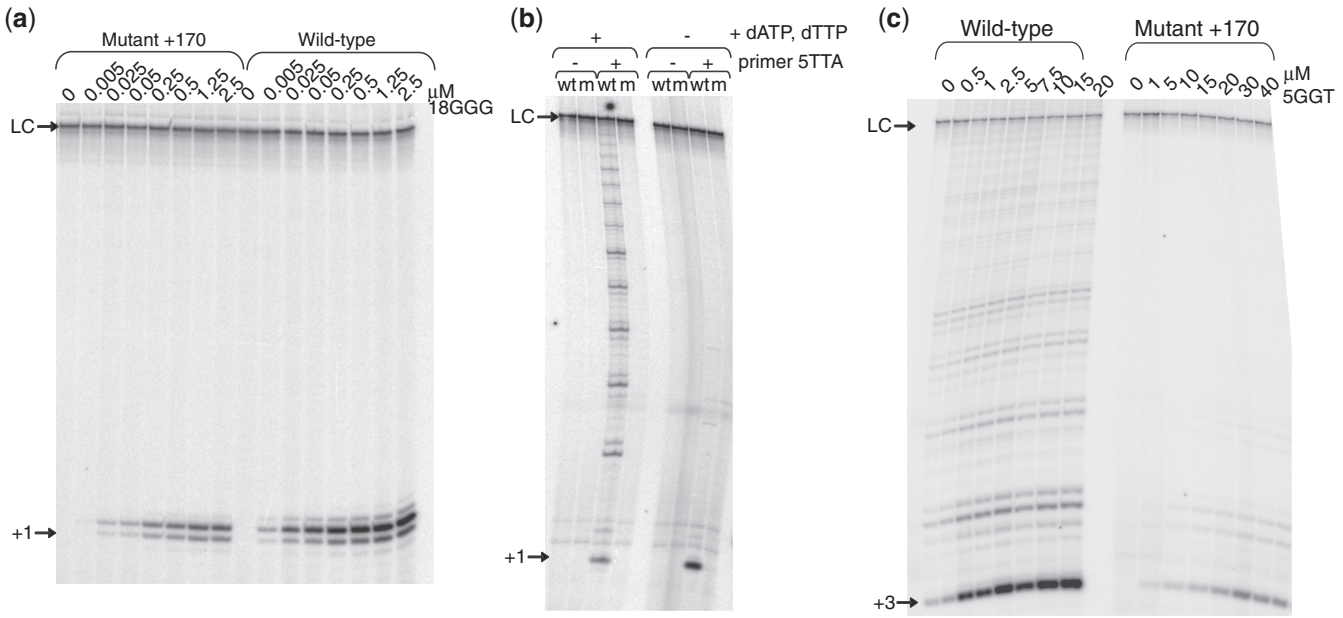

Figure 4. Increased K_m of mutant +170 is not attributable to a defect in translocation rate or interaction with 5′-end of primer. (**a**) Direct telomerase activity assay with wt or mutant recombinant telomerase using a titration of primer 18GGG, in the presence of ^{32}P-dTTP and no other nucleotide, in order to measure activity in the absence of translocation. LC: labelled 100 nt oligonucleotide as a recovery and loading control; +1: primer plus 1 nucleotide. (**b**) Activity assay in the presence or absence of primer 5TTA (5′-GGTTA-3′, 50 μM), with ^{32}P-dGTP alone (right four lanes) or ^{32}P-dGTP, dATP and dTTP (left four lanes), using wt or mutant +170 (m) recombinant telomerase. (**c**) Activity assay using a titration of primer 5GGT and recombinant telomerase. LC: labelled 100 nt oligonucleotide as a recovery and loading control; +3: primer plus 3 nt.

thymidines to the primer followed by dissociation, i.e. it does not include the translocation step (Figure 4a; see Figure 6a for primer-template alignment). The K_m for mutant +170 in this assay was 360 ± 30 nM and that of wt enzyme 57 ± 12 nM, similar to that of a processive reaction (Table 2). These data demonstrate that: (i) the translocation rate does not contribute greatly to the primer K_m of recombinant wt telomerase and (ii) mutant +170 retains a 6-fold defect in K_m in comparison to wt, indicating that translocation contributes at most a small amount to its increased K_m.

Crosslinking of a DNA primer to the TEN domain of *Tetrahymena* TERT has been observed using primers with photocrosslinkable substitutions at the 5′-end of a 20 nt primer (11,19), suggesting that TEN binds to the primer at an anchor site far upstream of the enzyme active site. To determine whether the K_m defect of mutant +170 reflects a defect in such interactions, we measured the K_m of recombinant human telomerase with shorter oligonucleotide substrates. Using primer 9GGG (5′-GGGTTA GGG-3′), the K_m of mutant +170 was ~5-fold higher than that of wt telomerase (Table 2). The primer 5TTA (5′-GG TTA-3′) was extended processively by wt telomerase but not extended by mutant +170 (Figure 4b). Primer 5GGT (5′-AGGGT-3′), which completely hybridizes with the RNA template, was extended by wt telomerase with a K_m of ~2.5 μM, whereas the K_m of mutant +170 with this primer was ~30 μM (Figure 4c). Thus the +170 mutation results in a defect that is independent of the presence of template-distal DNA primer sequences.

To determine whether the DNA binding defect exhibited by overexpressed cellular +170 telomerase (Table 3) involved binding to the 5′-end of the 18 nt primers, we also measured K_d of a 12-nt oligonucleotide (Bio-12GGG) using the direct primer pulldown assay. Mutant +170 demonstrated an even more dramatic defect in affinity for this primer than for the 18-nt primers, indicating that neither the K_m nor K_d defects of this mutant reflect interactions with the nucleotides at the 5′-end of an 18-nt primer.

hTERT mutant +170 is defective in nucleotide polymerization, particularly opposite position 51 of the template

Since K_m is a measure of total enzyme activity, it is likely that many kinetic parameters contribute to this value. For example, since DNA dissociation rate varies at each template position (47), it is possible that polymerization rate (k_{pol}) also varies across the telomerase template; this has not previously been tested. We therefore propose the telomerase kinetic scheme in Figure 5, illustrated for one round of addition of a TTAGGG repeat. The scheme includes rate constants for association and dissociation of primers of six permutations (e.g. $k_{on(GGG)}$ and $k_{off(GGG)}$), polymerization at the six positions (e.g. k_{pol-1}), and translocation (k_{trans}). The 21 rate constants shown here, plus nucleotide association constants and possible protein conformational changes that are not shown, contribute to the overall K_m for processive extension of a primer. In non-processive reactions including a single dNTP, such as that in Figure 4a, the K_m would represent a portion of this scheme, illustrated by the dashed box in Figure 5 for primer 18GGG.

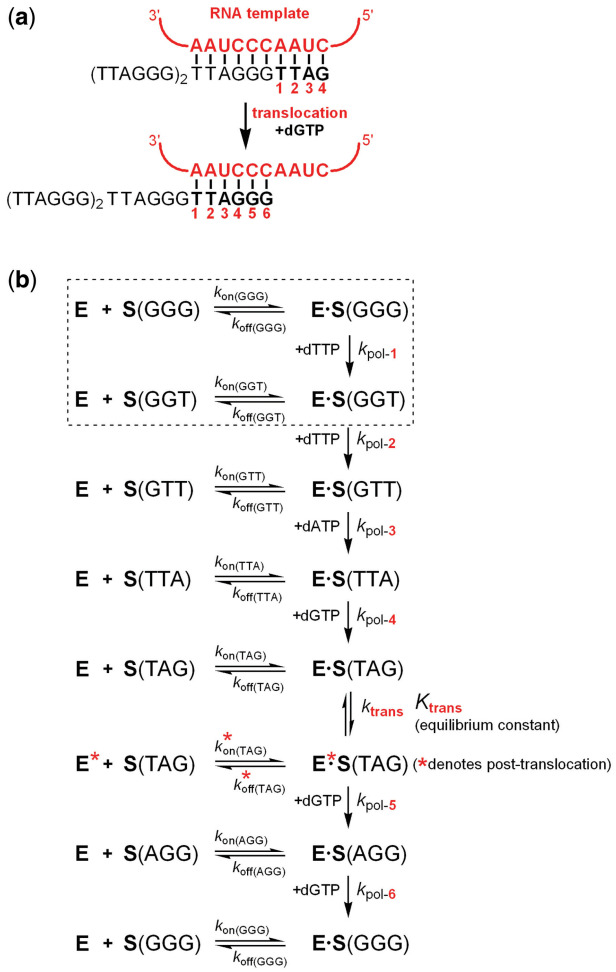

Figure 5. Proposed kinetic scheme for human telomerase. (**a**) Alignment of an elongated 18 nt DNA primer (black) with the RNA template (red) before (top) and after (bottom) translocation and addition of two Gs. Numbers 1–6 are assigned to each position of nucleotide addition within a single telomeric repeat. (**b**) Proposed kinetic scheme for telomerase. E = telomerase, S = DNA substrate, with 3′-permutation of each DNA primer in parenthesis. ES = telomerase–DNA complex. It has been demonstrated that the dissociation rate (k_{off}) of a particular DNA sequence is the same whether that DNA is the substrate or product of extension (47), so only one k_{off} has been included for each sequence. Note that the rate constant for translocation (k_{trans}) is potentially composed of at least two other rate constants, for RNA–DNA dissociation and realignment, respectively (50). Protein conformational changes and nucleotide association constants are not shown in this scheme. The dashed box indicates the portion of this scheme measured in a reaction with 18GGG as the DNA primer and dTTP as the only nucleotide.

To measure k_{pol-1} to k_{pol-6}, we used a set of six 18-nt primers representing the different repeat permutations, as shown in Figure 6a. Reactions including a single radiolabelled nucleotide were carried out at saturating DNA and dNTP concentrations for 3 h (Figure 6b), which is within the linear range of the reaction. The reactions shown in Figure 6b and Table 4 included DNA concentrations of 2 μM; the results did not change at 5 μM primer concentration, confirming that the DNA was saturating (data not shown). The rate of these reactions therefore represents the rate of addition of nucleotides; since we cannot distinguish between measurement of k_{pol} and rates of protein conformational change (since we do not know which is rate limiting), we have termed the resulting rate constant k_{obs} (Table 4). The k_{obs} at each position is similar for recombinant telomerase and telomerase overexpressed in 293T cells; note that the units are h^{-1}, demonstrating that telomerase is a slow enzyme. For wt telomerase, k_{obs} varies by a factor of 10–20, with the slowest addition being at position 5 (opposite RNA nucleotide 51, see Figure 6a) and the fastest at position 1 (opposite RNA nucleotide 49). Note that these differences do not correlate with the ~100-fold differences in enzyme dissociation measured for these six primers (47), indicating that primer dissociation is not rate-limiting in this experiment.

Mutant +170 demonstrated a reduced k_{obs} at each template position (Figure 6b, Table 4). Most strikingly, there was a complete lack of detectable addition to primer 18TAG when using recombinant telomerase (Figure 6b, top panel). This reflects an inability to copy position 51 of the RNA template and thus an inability to add the second G in the repeat TTAGGG. This was confirmed by the pattern of addition to primer 18TTA; mutant +170 telomerase is able to add a single G to this primer, but not the second G. Telomerase reconstituted in 293T cells presumably retained more contaminating nucleases and polymerases after purification, since it produced more bands representing nuclease activity or non-templated primer elongation (Fig. 6b, lower panel, bands without asterisks), which complicates interpretation of these reactions. In particular, a band of slightly slower mobility is obscuring the extension products of primer 18TAG. Nevertheless, the trend for a reduction in k_{obs} for mutant +170 reflects that of recombinant telomerase, and this appears to be most dramatic with primer 18TAG.

Since primers 18TTA and 18TAG can each hybridize to two positions on the RNA template, it is theoretically possible that they preferentially hybridize at the template 5′-end. This is unlikely, since primer 18TAG displays a monophasic dissociation rate that reflects binding to the 3′-end of the template (47). If true, however, this would mean that an inability to add the second G could be due to a defect in translocation rather than a defect in addition opposite RNA position 51. To address this, we made use of a primer with 3 nt changed such that the 3′-end of the primer can only align at the 3′-end of the template (primer 18ACT; see Figure 6a, bottom). wt telomerase was able to processively extend this primer almost as well as primer 18GGG (Figure 6c). This indicates that human telomerase does have the ability to utilize the 3′-end of its RNA template, and thus an inability to extend primer 18TAG likely represents a polymerization defect rather than a translocation defect. As predicted, mutant +170 is unable to add nucleotides to primer 18ACT.

The rate constants representing nucleotide association are not shown in Figure 5 for simplicity, but may contribute to final K_m values. As a start towards measuring these affinities, we titrated dGTP in a non-processive reaction using primer 18TTA (Figure 6d). The K_m for dGTP of wt recombinant telomerase was 1.3 ± 0.4 μM, while that of mutant +170 was ~3-fold higher at 4.2 ± 1.8 μM.

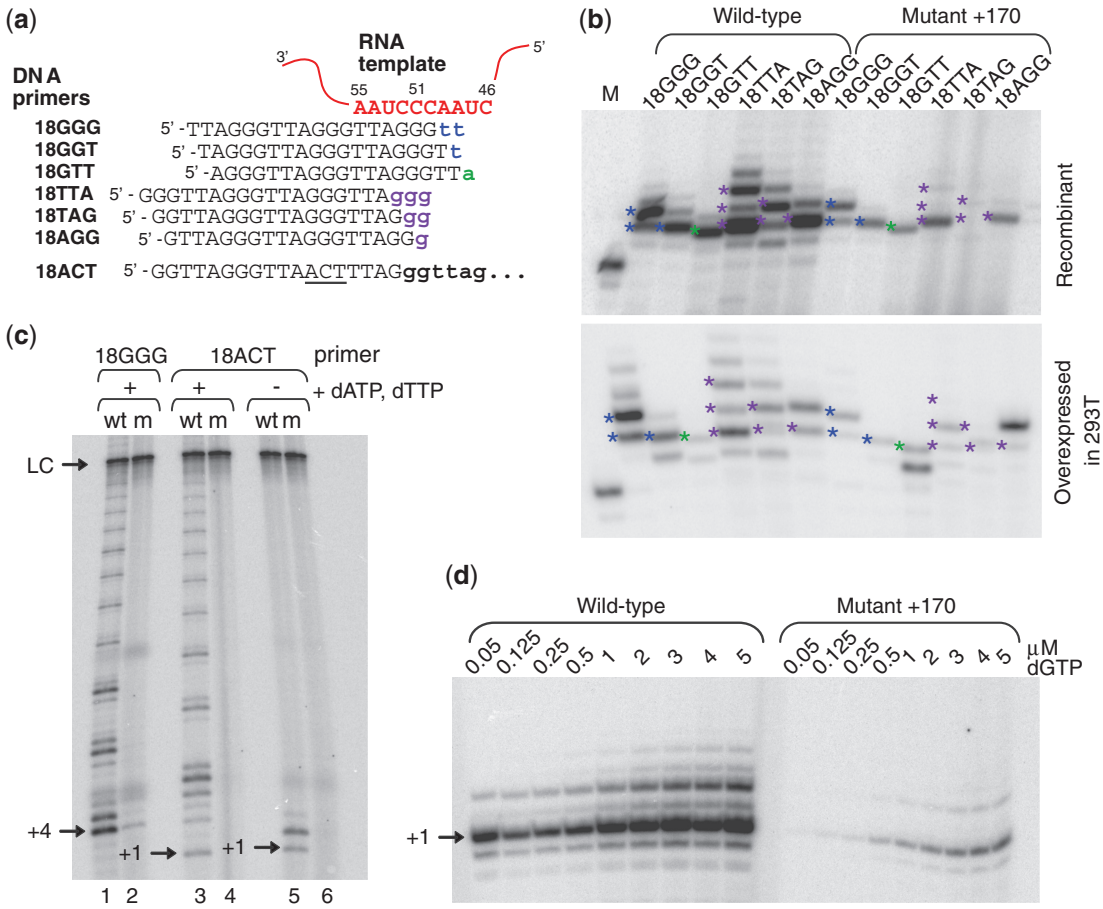

Figure 6. hTERT mutant +170 is defective in nucleotide polymerization, particularly opposite position 51 of the template. (**a**) Schematic of alignment of permuted 18 nt DNA primers with the RNA template. Nucleotide position numbers of the template within hTR are shown. Primer DNA sequence is in black uppercase; nucleotides added in reactions with a single radiolabelled nucleotide are indicated in coloured bold lower case. In primer 18ACT, the region of mismatch with the RNA template is underlined. (**b**) Activity assay measuring polymerization rate at each position of the RNA template, using recombinant telomerase (top panel) or telomerase overexpressed in 293T cells (bottom panel). Assays included the DNA primers indicated, and a single radiolabelled nucleotide: ^{32}P-dTTP (with 18GGG and 18GGT), ^{32}P-dATP (with 18GTT) or ^{32}P-dGTP (with 18TTA, 18TAG and 18AGG). Positions of templated additions of nucleotides are indicated with coloured asterisks. M = marker, ^{32}P end labelled 18GGG primer. (**c**) Extension of primer 18ACT by wild type (wt) and mutant +170 (m) recombinant telomerase, in processive (lanes 3 and 4) or non-processive (lanes 5 and 6) reactions. LC: labelled 100 nt oligonucleotide as a recovery and loading control; +1: primer plus 1 nt; +4: primer plus 4 nt. (**d**) Titration of dGTP in a non-processive reaction with primer 18TTA. The specific activity of the ^{32}P-dGTP was kept constant over all dGTP concentrations. +1: primer plus 1 nt.

Table 4. k_{obs} using DNA primers with each of six repeat permutations, with wt recombinant and overexpressed hTERT and mutant +170

Primer	Sequence	k_{obs} (h^{-1})					
		Recombinant			Overexpressed in 293T		
		wt	+170	Fold defect	wt	+170	Fold defect
18GGG	$(TTAGGG)_3$	2.7 ± 1.4	0.7 ± 0.5	4	2.9 ± 1.8	0.8 ± 0.5	4
18GGT	$(TAGGGT)_3$	1.7 ± 0.7	0.5 ± 0.2	3	2.5 ± 0.8	0.4 ± 0.2	6
18GTT	$(AGGGTT)_3$	1.3 ± 0.7	0.3 ± 0.2	4	1.8 ± 0.5	1.9 ± 1.1	1
18TTA	$(GGGTTA)_3$	0.9 ± 0.2	0.09 ± 0.02	10	0.7 ± 0.2	0.2 ± 0.1	3
18TAG	$(GGTTAG)_3$	0.21 ± 0.03	<0.006	>35	0.15 ± 0.06	n.q.	n.q.
18AGG	$(GTTAGG)_3$	0.41 ± 0.06	0.06 ± 0.01	7	0.34 ± 0.09	0.15 ± 0.12	2
	Overall	0.25 ± 0.09	0.029 ± 0.006	9	n.d.	n.d.	n.d.

The rates in the first six rows were calculated for reactions including a single radiolabelled nucleotide, i.e. non-processive reactions. The rate in the bottom row represents a processive reaction with the primer 18GGG. Results are the mean ± standard deviation of three experiments.
n.d., not determined; n.q., not quantifiable due to contaminating products.

Therefore it is possible that this mutation affects the ability of nucleotides to enter the enzyme active site, possibly via an allosteric interaction of the TEN domain with the active site. However, this 3-fold defect in K_m for dGTP is insufficient to explain the >35-fold defect in addition to primer 18TAG; furthermore, the latter reaction was carried out at a dGTP concentration of 10 μM. Thus the data in Figure 6b and Table 4 point to a defect of mutant +170 in k_{pol} (particularly k_{pol-5}) and/or a defect in protein conformational changes during catalysis.

Homology model of the human TEN domain with a docked DNA primer

The crystal structure of the *Tetrahymena* TEN domain was used to perform homology modelling of the hTERT TEN domain using a threading technique (Figure 7b). Although of low sequence similarity, the essential features of the human TEN domain model and the *Tetrahymena* structure are very similar; in particular, the predicted DNA binding groove and the region mutated in this study are highly similar (Figure 7b, red and yellow, respectively). This model is also similar to a previously published homology model of the human TEN domain (48). The regions of most difference in all the models are the poorly conserved loops (Supplementary Figure S4).

The 3 nt DNA primer 5′-TTA-3′ was docked into the TEN domain model using the HEX programme (42). The top-scoring solution was positioned with its 3′-end in the pocket formed by amino acids 170–175, and showed polar interactions with Val81, Asn95, Lys94, Tyr176 and Gln177 (Supplementary Figure S5 and Table S2). The DNA substrate is also positioned in a way that the further addition of bases to the 5′-end could lead to interactions with residue Pro188.

During extension, the 3′-end of the DNA primer is predicted to form a duplex with the RNA template. The addition of the complementary RNA base pairs to the docked DNA primer resulted in a steric clash between the RNA and a large loop in the TEN domain. However, it is plausible that this loop is sufficiently flexible to move out of the way, allowing interaction with an RNA–DNA duplex (Supplementary Figure S6).

DISCUSSION

Kinetic analyses of telomerase extension using the hTERT TEN domain mutant +170 has demonstrated that a major defect of this mutant is in nucleotide addition opposite position 51 of the RNA template. This mutant also exhibits a defect in affinity for an 18 nt DNA primer, corroborating previous data implicating the TEN domain as a contributor to DNA binding affinity. However, our results demonstrate that the defect in catalysis of mutant +170 is *independent* of its defect in DNA binding, since catalytic rate measurements were carried out at saturating DNA concentration. These observations expand the numerous functions of this important region of hTERT.

The observed catalytic defect may reflect a difference in the actual polymerization rate of telomerase at this position, or, since these amino acids are not part of the catalytic triad of aspartates, a protein conformational change during this step of catalysis. The latter conclusion is supported by the finding of a possible conformational change in the vicinity of the TEN domain in a mutant of the nearby amino acid Q169 (30), although it should be emphasized that we are proposing a defect in a conformational change *during* catalysis rather than in the steady-state conformation of the enzyme; the former would be considerably more difficult to measure.

Together with previous data demonstrating that amino acids in this vicinity of *Tetrahymena* TERT have the ability to crosslink to a DNA primer (19,28), our data suggest that this region of the TEN domain is involved in positioning the 3′-end of the primer in the active site (Figure 7a). Docking of the DNA primer in our human TEN homology model supports this proposition (Supplementary Figure S5). Conformational changes in the enzyme are undoubtedly occurring as the RNA–DNA duplex is realigned with the active site after addition of each dNTP, and we propose that the TEN domain plays a key role in mediating these. Amino acids 170–175 are particularly involved in the transition from –TAG to –TAGG; this transition may be the one requiring the greatest conformational change, or possibly the other five transitions are primarily mediated by other amino acids. The former possibility is supported by the finding that an amino acid in a completely different region of *Tetrahymena* TERT also leads to a defect in addition of the second G in the telomeric repeat (49). This is also the position of slowest addition (Table 4).

Mutant +170 affects nucleotide addition to some extent at every position of the RNA template. This indicates that these amino acids remain in the vicinity of the telomerase active site throughout the addition cycle. Furthermore, the DNA binding affinity provided by these amino acids is also localized to the 3′-end of the primer. We postulate that the two defects, while functionally separable, are related in that they both result from reduced binding of amino acids 170–175 to the 3′-end of the DNA. This region of the TEN domain is therefore not involved in the classical 'anchor site' at the 5′-end of the DNA primer. In *Tetrahymena* TERT, amino acid W187 remains close to DNA at the 3′-template boundary throughout the addition cycle (28). Combining these two observations results in a model whereby the distance between these amino acids increases over the addition cycle (Figure 7a). Since the predicted length of the template RNA–primer DNA duplex is ~27 Å, the distance between W187 and Q168 in *Tetrahymena* TERT is ~24 Å, and the corresponding distance in the human TEN model is also ~24 Å, we propose that the structures in Figure 7b represent the 'stretched' state of the TEN domain just prior to translocation. Our model (illustrated in Figure 7a) is a refinement of previous models for the function of the TEN domain in that we propose: (i) the conformational change may be within the TEN domain itself, rather than between the TEN domain and the rest of the protein (28), and (ii) the conformational change is one

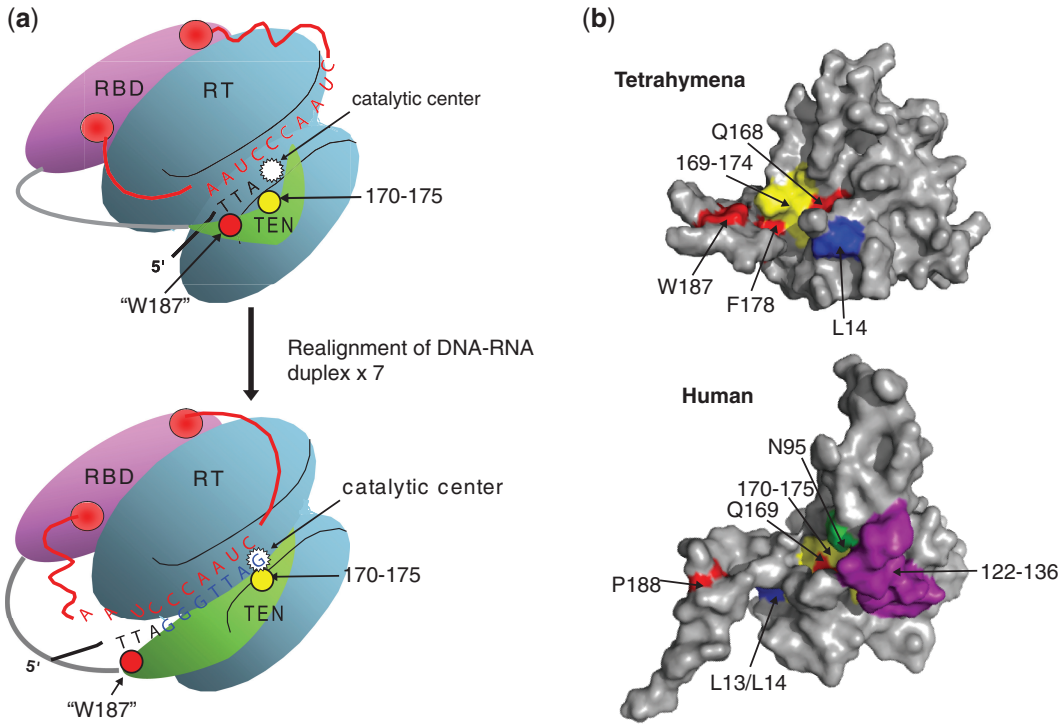

Figure 7. Models of the location, structure and function of hTERT region 170–175. (**a**) Proposed function of hTERT amino acids 170–175 in positioning 3′-end of primer in active site. According to this model, this region of the TEN domain (yellow circle) is positioned close to the enzyme active site (white star). As each nucleotide is added to a DNA primer ending in—TTA, the DNA–RNA duplex becomes repositioned so the new 3′-end is in the active site. Depicted in red is the hTERT amino acid homologous to *Tetrahymena* W187; the latter has been shown to interact with a DNA nucleotide close to the template boundary (28). See text for more detail. (**b**) Top: crystal structure of the TEN domain from *Tetrahymena* TERT (19). The amino acids homologous to hTERT region 170–175 are shown in yellow [from sequence alignment in ref. (56)]. Amino acids involved in crosslinking to a DNA primer (Q168, F178, W187) are red (19,28). An amino acid involved in repeat addition processivity (L14) is blue (31). Bottom: homology model of the TEN domain of human TERT. The amino acids mutated in this study (170–175) are in yellow. Amino acids homologous to those shown in *Tetrahymena* to crosslink to a primer are shown in red (Q169, P188). hTERT region 122–136 is coloured purple [part of the 'DAT' domain (32)]. Amino acids involved in repeat addition processivity (L13 and L14) are blue (31). N95, shown to be involved in DNA binding, is green (29). Figures were constructed using PYMOL (57). Note that the colours used in this figure bear no relationship to those used in Figure 1.

occurring during nucleotide addition rather than during translocation as previously proposed (31).

The extent of the DNA affinity defect of overexpressed cellular mutant +170 (500–1000-fold for 18-nt primers) is the most significant observed so far for the human telomerase TEN domain (24,27,29,30,50). Interestingly, this DNA binding defect was barely detectable using recombinant mutant +170 telomerase expressed in RRL. This may explain discrepancies in the literature regarding the extent of DNA affinity contributed by this region of the hTERT TEN domain (24,30).

DNA nucleotides 12–24 nt upstream of the primer 3′-end have been shown to crosslink to the *Tetrahymena* TEN domain (11,19) and provide extra binding affinity of DNA to the isolated human TEN domain (24). It is therefore likely that other amino acids in the TEN domain contribute to the classical telomerase 'anchor site' at the 5′-end of the primer (13–15). The intervening nucleotides may 'loop-out' during processive elongation as previously proposed (13,14), with the TEN domain functioning to tether the primer 5′-end to the site of nucleotide addition.

DNA affinity is known to be a determinant of telomerase repeat addition processivity (51). In the case of hTERT mutant +170, decreased RAP is not rescued at high primer concentration (Supplementary Figure S1), suggesting that the decrease in RAP is a consequence of failure to efficiently copy an entire repeat, rather than due to the DNA affinity defect of this mutant. Mutation of hTERT amino acids L13 and L14 also leads to a decrease in RAP without a decrease in DNA affinity (31). It was proposed that the decrease in RAP of the latter mutant is due to altered conformational changes at the translocation step, although a specific defect in extension of primers pairing near the 3′-end of the template was also observed (31).

Previous studies on the biochemical properties of mutations in the TEN domain point to a number of functions for this region. These data, in combination with our new results, lead us to propose that the hTERT TEN domain comprises at least three functional domains (Figure 7b):

(i) A DNA binding groove that is essential for DNA affinity (Figure 7b, yellow, red and green). This groove seems to be conserved between species, since it was first identified in the structure of the *Tetrahymena* TEN domain, and can be crosslinked to DNA primers in this species (19,28). In human TERT, N95 has been shown to directly contribute

to affinity (29) and modelling supports a direct interaction with the DNA primer (Supplementary Figure S5). Our modelling data indicate that the 3′-end of the DNA is bound by the 170–175 pocket, while the 5′-end of the DNA extends towards P188 (Supplementary Figure S5).

(ii) An overlapping region that is involved specifically in conformational changes during nucleotide addition, the function elucidated in this study (Figure 7b, yellow and blue). It remains possible that part of this region (blue, L13 and L14) instead forms an interaction with a different part of TERT that is important during translocation (31).

(iii) A protein–protein interaction domain, part of the previously defined N-DAT domain (32), that is involved in telomerase recruitment to the telomere (Figure 7b, purple). Mutation of amino acids 122–136 in hTERT impacts little on enzyme activity, processivity, K_m, or primer K_d as measured by a direct binding assay (29, this study). Instead, there is evidence that targeting these mutant telomerase molecules to the telomere overcomes their defect *in vivo* (52,53). The role of these amino acids in interacting with other proteins is supported by their location on the surface of our homology model (Figure 7b, purple).

Other proposed functions of the hTERT TEN domain include low-affinity RNA binding that has not been localized to particular amino acids (18,23,54,55) and a nucleolar localization domain in a region not shared with *Tetrahymena* TERT (45).

Compared to many other enzymes, telomerase has a complicated mechanism of action that involves many movements of the RNA template and DNA primer relative to the enzyme's active site. Not surprisingly, K_m is not an accurate prediction of the finer mechanistic details of telomerase. This study represents one of the first attempts to assign quantitative values to multiple kinetic parameters of human telomerase. This process has uncovered the importance of an essential N-terminal domain of the protein in events at the enzyme's active site.

SUPPLEMENTARY DATA

Supplementary Data are available at NAR Online.

ACKNOWLEDGEMENTS

We thank Christopher Counter (Duke University, USA) for the hTERT-NAAIRS-pBabehygro constructs, Jamie Sperger and Tom Cech (University of Colorado at Boulder, USA) for the hTR transcription plasmid, Kathleen Collins (University of California at Berkeley, USA) for the U3-hTR plasmid, Lorel Colgin and Roger Reddel (Children's Medical Research Institute, Australia) for the hTERT plasmid and Natsuki Sasaki, Josh Stern and John Mitry for technical assistance.

FUNDING

Wellcome Trust Senior Research Fellowship (GR066727MA to T.M.B.); a Cancer Institute NSW Career Development and Support Fellowship (to T.M.B.); a National Health and Medical Research Council postdoctoral fellowship (to A.S.N.); an Australian Research Council Federation Fellowship (to M.W.P.); National Health and Medical Research Council project grants (to T.M.B. and S.B.C.). Funding for open access charge: Children's Medical Research Institute.

Conflict of interest statement. None declared.

REFERENCES

1. McEachern,M.J., Krauskopf,A. and Blackburn,E.H. (2000) Telomeres and their control. *Annu. Rev. Genet.*, **34**, 331–358.
2. Greider,C.W. and Blackburn,E.H. (1985) Identification of a specific telomere terminal transferase activity in *Tetrahymena* extracts. *Cell*, **43**, 405–413.
3. Shay,J.W. and Bacchetti,S. (1997) A survey of telomerase activity in human cancer. *Eur. J. Cancer*, **33**, 787–791.
4. Hahn,W.C., Stewart,S.A., Brooks,M.W., York,S.G., Eaton,E., Kurachi,A., Beijersbergen,R.L., Knoll,J.H., Meyerson,M. and Weinberg,R.A. (1999) Inhibition of telomerase limits the growth of human cancer cells. *Nat. Med.*, **5**, 1164–1170.
5. Zhang,X., Mar,V., Zhou,W., Harrington,L. and Robinson,M.O. (1999) Telomere shortening and apoptosis in telomerase-inhibited human tumor cells. *Genes Dev.*, **13**, 2388–2399.
6. Lingner,J., Hughes,T.R., Shevchenko,A., Mann,M., Lundblad,V. and Cech,T.R. (1997) Reverse transcriptase motifs in the catalytic subunit of telomerase. *Science*, **276**, 561–567.
7. Greider,C.W. and Blackburn,E.H. (1987) The telomere terminal transferase of Tetrahymena is a ribonucleoprotein enzyme with two kinds of primer specificity. *Cell*, **51**, 887–898.
8. Weinrich,S.L., Pruzan,R., Ma,L., Ouellette,M., Tesmer,V.M., Holt,S.E., Bodnar,A.G., Lichtsteiner,S., Kim,N.W., Trager,J.B. *et al.* (1997) Reconstitution of human telomerase with the template RNA component hTR and the catalytic protein subunit hTRT. *Nat. Genet.*, **17**, 498–502.
9. Collins,K. and Gandhi,L. (1998) The reverse transcriptase component of the *Tetrahymena* telomerase ribonucleoprotein complex. *Proc. Natl Acad. Sci. USA*, **95**, 8485–8490.
10. Lee,M.S. and Blackburn,E.H. (1993) Sequence-specific DNA primer effects on telomerase polymerization activity. *Mol. Cell. Biol.*, **13**, 6586–6599.
11. Finger,S.N. and Bryan,T.M. (2008) Multiple DNA-binding sites in *Tetrahymena* telomerase. *Nucleic Acids Res.*, **36**, 1260–1272.
12. Lue,N.F. and Peng,Y. (1998) Negative regulation of yeast telomerase activity through an interaction with an upstream region of the DNA primer. *Nucleic Acids Res.*, **26**, 1487–1494.
13. Morin,G.B. (1991) Recognition of a chromosome truncation site associated with α-thalassaemia by human telomerase. *Nature*, **353**, 454–456.
14. Harrington,L.A. and Greider,C.W. (1991) Telomerase primer specificity and chromosome healing. *Nature*, **353**, 451–454.
15. Collins,K. and Greider,C.W. (1993) *Tetrahymena* telomerase catalyzes nucleolytic cleavage and nonprocessive elongation. *Genes Dev.*, **7**, 1364–1376.
16. Friedman,K.L. and Cech,T.R. (1999) Essential functions of amino-terminal domains in the yeast telomerase catalytic subunit revealed by selection for viable mutants. *Genes Dev.*, **13**, 2863–2874.
17. Xia,J., Peng,Y., Mian,I.S. and Lue,N.F. (2000) Identification of functionally important domains in the N-terminal region of telomerase reverse transcriptase. *Mol. Cell. Biol.*, **20**, 5196–5207.
18. Moriarty,T.J., Huard,S., Dupuis,S. and Autexier,C. (2002) Functional multimerization of human telomerase requires an

RNA interaction domain in the N terminus of the catalytic subunit. *Mol. Cell. Biol.*, **22**, 1253–1265.
19. Jacobs,S.A., Podell,E.R. and Cech,T.R. (2006) Crystal structure of the essential N-terminal domain of telomerase reverse transcriptase. *Nat. Struct. Mol. Biol.*, **13**, 218–225.
20. Jacobs,S.A., Podell,E.R., Wuttke,D.S. and Cech,T.R. (2005) Soluble domains of telomerase reverse transcriptase identified by high-throughput screening. *Protein Sci.*, **14**, 2051–2058.
21. O'Connor,C.M., Lai,C.K. and Collins,K. (2005) Two purified domains of telomerase reverse transcriptase reconstitute sequence-specific interactions with RNA. *J. Biol. Chem.*, **280**, 17533–17539.
22. Beattie,T.L., Zhou,W., Robinson,M.O. and Harrington,L. (2001) Functional multimerization of the human telomerase reverse transcriptase. *Mol. Cell. Biol.*, **21**, 6151–6160.
23. Moriarty,T.J., Marie-Egyptienne,D.T. and Autexier,C. (2004) Functional organization of repeat addition processivity and DNA synthesis determinants in the human telomerase multimer. *Mol. Cell. Biol.*, **24**, 3720–3733.
24. Sealey,D.C., Zheng,L., Taboski,M.A., Cruickshank,J., Ikura,M. and Harrington,L.A. (2010) The N-terminus of hTERT contains a DNA-binding domain and is required for telomerase activity and cellular immortalization. *Nucleic Acids Res.*, **38**, 2019–2035.
25. Lue,N.F. (2005) A physical and functional constituent of telomerase anchor site. *J. Biol. Chem.*, **280**, 26586–26591.
26. Lue,N.F. and Li,Z. (2007) Modeling and structure function analysis of the putative anchor site of yeast telomerase. *Nucleic Acids Res.*, **35**, 5213–5222.
27. Moriarty,T.J., Ward,R.J., Taboski,M.A. and Autexier,C. (2005) An anchor site-type defect in human telomerase that disrupts telomere length maintenance and cellular immortalization. *Mol. Biol. Cell*, **16**, 3152–3161.
28. Romi,E., Baran,N., Gantman,M., Shmoish,M., Min,B., Collins,K. and Manor,H. (2007) High-resolution physical and functional mapping of the template adjacent DNA binding site in catalytically active telomerase. *Proc. Natl Acad. Sci. USA*, **104**, 8791–8796.
29. Wyatt,H.D., Lobb,D.A. and Beattie,T.L. (2007) Characterization of physical and functional anchor site interactions in human telomerase. *Mol. Cell. Biol.*, **27**, 3226–3240.
30. Wyatt,H.D., Tsang,A.R., Lobb,D.A. and Beattie,T.L. (2009) Human telomerase reverse transcriptase (hTERT) Q169 is essential for telomerase function in vitro and in vivo. *PLoS ONE*, **4**, e7176.
31. Zaug,A.J., Podell,E.R. and Cech,T.R. (2008) Mutation in TERT separates processivity from anchor-site function. *Nat. Struct. Mol. Biol.*, **15**, 870–872.
32. Armbruster,B.N., Banik,S.S., Guo,C., Smith,A.C. and Counter,C.M. (2001) N-terminal domains of the human telomerase catalytic subunit required for enzyme activity *in vivo*. *Mol. Cell. Biol.*, **21**, 7775–7786.
33. Nakamura,T.M., Morin,G.B., Chapman,K.B., Weinrich,S.L., Andrews,W.H., Lingner,J., Harley,C.B. and Cech,T.R. (1997) Telomerase catalytic subunit homologs from fission yeast and human. *Science*, **277**, 955–959.
34. Kilian,A., Bowtell,D.D., Abud,H.E., Hime,G.R., Venter,D.J., Keese,P.K., Duncan,E.L., Reddel,R.R. and Jefferson,R.A. (1997) Isolation of a candidate human telomerase catalytic subunit gene, which reveals complex splicing patterns in different cell types. *Hum. Mol. Genet.*, **6**, 2011–2019.
35. Harrington,L., Zhou,W., McPhail,T., Oulton,R., Yeung,D.S., Mar,V., Bass,M.B. and Robinson,M.O. (1997) Human telomerase contains evolutionarily conserved catalytic and structural subunits. *Genes Dev.*, **11**, 3109–3115.
36. Bryan,T.M., Marusic,L., Bacchetti,S., Namba,M. and Reddel,R.R. (1997) The telomere lengthening mechanism in telomerase-negative immortal human cells does not involve the telomerase RNA subunit. *Hum. Mol. Genet.*, **6**, 921–926.
37. Zaug,A.J. and Cech,T.R. (1995) Analysis of the structure of Tetrahymena nuclear RNAs *in vivo*: telomerase RNA, the self-splicing rRNA intron, and U2 snRNA. *RNA*, **1**, 363–374.
38. Colgin,L.M., Wilkinson,C., Englezou,A., Kilian,A., Robinson,M.O. and Reddel,R.R. (2000) The hTERTα splice variant is a dominant negative inhibitor of telomerase activity. *Neoplasia*, **2**, 426–432.
39. Fu,D. and Collins,K. (2003) Distinct biogenesis pathways for human telomerase RNA and H/ACA small nucleolar RNAs. *Mol. Cell*, **11**, 1361–1372.
40. Cohen,S.B. and Reddel,R.R. (2008) A sensitive direct human telomerase activity assay. *Nat. Methods*, **5**, 355–360.
41. Laskowski,R.A., Moss,D.S. and Thornton,J.M. (1993) PROCHECK-A program to check the stereochemical quality of protein structures. *J. Appl. Crystallogr.*, **26**, 283–291.
42. Ritchie,D.W. and Kemp,G.J. (2000) Protein docking using spherical polar Fourier correlations. *Proteins*, **39**, 178–194.
43. Banik,S.S., Guo,C., Smith,A.C., Margolis,S.S., Richardson,D.A., Tirado,C.A. and Counter,C.M. (2002) C-terminal regions of the human telomerase catalytic subunit essential for in vivo enzyme activity. *Mol. Cell. Biol.*, **22**, 6234–6246.
44. Wilson,I.A., Haft,D.H., Getzoff,E.D., Tainer,J.A., Lerner,R.A. and Brenner,S. (1985) Identical short peptide sequences in unrelated proteins can have different conformations: a testing ground for theories of immune recognition. *Proc. Natl Acad. Sci. USA*, **82**, 5255–5259.
45. Yang,Y., Chen,Y., Zhang,C., Huang,H. and Weissman,S.M. (2002) Nucleolar localization of hTERT protein is associated with telomerase function. *Exp. Cell Res.*, **277**, 201–209.
46. Huard,S., Moriarty,T.J. and Autexier,C. (2003) The C terminus of the human telomerase reverse transcriptase is a determinant of enzyme processivity. *Nucleic Acids Res.*, **31**, 4059–4070.
47. Wallweber,G., Gryaznov,S., Pongracz,K. and Pruzan,R. (2003) Interaction of human telomerase with its primer substrate. *Biochemistry*, **42**, 589–600.
48. Lee,J.H., Hamilton,M., Gleeson,C., Caragea,C., Zaback,P., Sander,J.D., Li,X., Wu,F., Terribilini,M., Honavar,V. *et al.* (2008) Striking similarities in diverse telomerase proteins revealed by combining structure prediction and machine learning approaches. *Pac. Symp. Biocomput.*, **13**, 501–512.
49. Miller,M.C., Liu,J.K. and Collins,K. (2000) Template definition by *Tetrahymena* telomerase reverse transcriptase. *EMBO J.*, **19**, 4412–4422.
50. Xie,M., Podlevsky,J.D., Qi,X., Bley,C.J. and Chen,J.J. (2010) A novel motif in telomerase reverse transcriptase regulates telomere repeat addition rate and processivity. *Nucleic Acids Res.*, **38**, 1982–1996.
51. Bryan,T.M., Goodrich,K.J. and Cech,T.R. (2000) A mutant of *Tetrahymena* telomerase reverse transcriptase with increased processivity. *J. Biol. Chem.*, **275**, 24199–24207.
52. Armbruster,B.N., Etheridge,K.T., Broccoli,D. and Counter,C.M. (2003) Putative telomere-recruiting domain in the catalytic subunit of human telomerase. *Mol. Cell. Biol.*, **23**, 3237–3246.
53. Armbruster,B.N., Linardic,C.M., Veldman,T., Bansal,N.P., Downie,D.L. and Counter,C.M. (2004) Rescue of an hTERT mutant defective in telomere elongation by fusion with hPot1. *Mol. Cell. Biol.*, **24**, 3552–3561.
54. Beattie,T.L., Zhou,W., Robinson,M.O. and Harrington,L. (2000) Polymerization defects within human telomerase are distinct from telomerase RNA and TEP1 binding. *Mol. Biol. Cell*, **11**, 3329–3340.
55. Bachand,F. and Autexier,C. (2001) Functional regions of human telomerase reverse transcriptase and human telomerase RNA required for telomerase activity and RNA-protein interactions. *Mol. Cell. Biol.*, **21**, 1888–1897.
56. Friedman,K.L., Heit,J.J., Long,D.M. and Cech,T.R. (2003) N-terminal domain of yeast telomerase reverse transcriptase: recruitment of Est3p to the telomerase complex. *Mol. Biol. Cell*, **14**, 1–13.
57. DeLano,W.L. (2002) *The PyMOL Molecular Graphics System*, DeLano Scientific, San Carlos, CA, USA, http://www.pymol.org.